Interaction of Dystrophin Rod Domain with Membrane Phospholipids

Elisabeth Le Rumeur, Yann Fichou, Sandrine Pottier, François Gaboriau, Corinne Rondeau-Mouro, Michel Vincent, Jacques Gallay, Arnaud Bondon

THE JOURNAL OF BIOLOGICAL CHEMISTRY
Vol. 278, No. 8, Issue of February 21, pp. 5993–6001, 2003

Printed in U.S.A.

Interaction of Dystrophin Rod Domain with Membrane Phospholipids

EVIDENCE OF A CLOSE PROXIMITY BETWEEN TRYPTOPHAN RESIDUES AND LIPIDS*

Received for publication, July 22, 2002, and in revised form, December 10, 2002
Published, JBC Papers in Press, December 11, 2002, DOI 10.1074/jbc.M207321200

Elisabeth Le Rumeur‡§, Yann Fichou‡, Sandrine Pottier‡, François Gaboriau¶, Corinne Rondeau-Mouro‡‖, Michel Vincent, Jacques Gallay**, and Arnaud Bondon‡‡**

*From the ‡Laboratoire de Résonance Magnétique Nucléaire en Biologie et Médecine (Unité Propre de Recherche de l'Enseignement Supérieur EA 2230), Faculté de Médecine, CS 34317, Rennes 35043 cedex, the ¶Groupe de Recherche en Thérapeutique anticancéreuse, CNRS FRE 2261, Faculté de Médecine, CS 34317, Rennes 35043 cedex, the ‡‡Laboratoire de Chimie Organométallique et Biologique, Unité Mixte de Recherche CNRS 6509, Rennes 35042 cedex, and the **Laboratoire pour l'Utilisation du Rayonnement Electromagnétique, Unité Mixte de Recherche CNRS 130, Centre Universitaire Paris Sud, BP 34, Orsay 91898, France*

Dystrophin is assumed to act via the central rod domain as a flexible linker between the amino-terminal actin binding domain and carboxyl-terminal proteins associated with the membrane. The rod domain is made up of 24 spectrin-like repeats and has been shown to modify the physical properties of lipid membranes. The nature of this association still remains unclear. Tryptophan residues tend to cluster at or near to the water-lipid interface of the membrane. To assess dystrophin rod domain-membrane interactions, tryptophan residues properties of two recombinant proteins of the rod domain were examined by ^{1}H NMR and fluorescence techniques in the presence of membrane lipids. F114 (residues 439–553) is a partly folded protein as inferred from ^{1}H NMR, tryptophan fluorescence emission intensity, and the excited state lifetime. By contrast, F125 (residues 439–564) is a folded compact protein. Tryptophan fluorescence quenching shows that both proteins are characterized by structural fluctuations with their tryptophan residues only slightly buried from the surface. In the presence of negatively charged small vesicles, the fluorescence characteristics of F125 change dramatically, indicating that tryptophan residues are in a more hydrophobic environment. Interestingly, these modifications are not observed with F114. Fluorescence quenching experiments confirm that tryptophan residues are shielded from the solvent in the complex F125 lipids by a close contact with lipids. The use of membrane-bound quenchers allowed us to conclude that dystrophin rod domain lies along the membrane surface and may be involved in a structural array comprising membrane and cytoskeletal proteins as well as membrane lipids.

Dystrophin is a filamentous 427-kDa protein whose deficiency is at the origin of Duchenne muscular dystrophy (1). The dystrophin molecule is composed of four domains: an actin-binding amino-terminal domain, a rod domain comprising 24 spectrin-like repeats, and a carboxyl-terminal end made up of cysteine-rich and dystroglycan-interacting domains anchoring the dystrophin molecule at the sarcolemma (2–4). The amino-terminal end (5) and a cluster of basic repeats of the rod domain (6) are clearly associated with F-actin, suggesting a lateral association between dystrophin and actin. All these associations point to a model of dystrophin acting as a flexible linker between the cytoskeleton and the extracellular matrix (7–9). However, it has also been observed that a repeat of the rod domain is able to modify the physical properties of lipid membranes containing anionic phospholipids (10). This result is consistent with the observation that, in the muscle of patients expressing genetic variants of dystrophin lacking the carboxyl-terminal end, the truncated dystrophin is nevertheless well localized at the sarcolemma (11–13). It is also compatible with the evidence for the presence of several repeats and hinges of the rod domain between the amino- and carboxyl-terminal ends, which is essential for a complete rescue of the dystrophic phenotype of the *mdx* mouse (14). The above studies lead to the view that the rod domain may target the dystrophin molecule onto the sarcolemma by a lateral association not only with F-actin but also with membrane phospholipids. Interactions with membrane lipids have already been reported for spectrin (15, 16) and have been shown to be involved in the shape regulation of the red cell membrane (17) and more recently in its membrane stability (18). Because spectrin and dystrophin belong to the same protein family, these results suggest a similar function for the two proteins.

However, the nature of the association of the rod domain with membrane lipids is still unclear. Tryptophan (Trp) residues are often involved in the membrane lipid association of interfacial proteins (19–21). Because several tryptophan residues are present in the rod domain repeats, we investigated these tryptophan properties and accessibility in two recombinant proteins of the rod domain, both in aqueous solution and in the presence of membrane lipids.

Calvert *et al.* (22) have made several interesting constructs of the second repeat of the human dystrophin rod domain involving a constant amino-terminal end but with variable carboxyl-terminal ends. In the present study, we chose to investigate two of these fragments, namely, the 114- and 125-residue-long proteins. Four Trp residues are present in the 114 protein, whereas there is one extra Trp residue in the 125 fragment (10). Although the 114 fragment does not fully fold,

* This work was supported in part by grants from the Association Française contre les Myopathies. The costs of publication of this article were defrayed in part by the payment of page charges. This article must therefore be hereby marked "*advertisement*" in accordance with 18 U.S.C. Section 1734 solely to indicate this fact.

‖ Supported by a fellowship from the Association Française contre les Myopathies.

§ To whom correspondence should be addressed. Tel.: 33-2-23-23-46-27; Fax: 33-2-23-23-46-06; E-mail: elisabeth.lerumeur@univ-rennes1.fr.

proteins longer than the 117 residues such as the 125 fragment are able to adopt a high percentage of α-helical content (22, 23).

We first used ^{1}H NMR spectroscopy, a technique that can give indications about the shielding of Trp residues in proteins. In addition, magnetization transfer between water and amide protons of Trp residues (24) may provide information about their respective accessibility to water. In addition, intrinsic fluorescence spectroscopy of tryptophan (Trp) is a valuable tool for studying the conformation of proteins by means of time-resolved fluorescence and quenching experiments (25–27). This can provide information about the environment of the indole ring of Trp, including its charge and polarity. Comparative Trp fluorescence spectroscopy of the two fragments of dystrophin rod domain proteins having different folding states can be used to determine the status of the Trp residues in these proteins and assess the possibility of their involvement in an interaction with membrane phospholipids.

MATERIALS AND METHODS

Protein Preparation—Proteins with lengths of 114 (F114) and 125 (F125)[1] residues of the second repeat of human dystrophin rod domain were prepared by expression in *Escherichia coli* (strain BL21(DE3)) of plasmids kindly provided by W. B. Gratzer (22). The amino terminus is common to the two proteins and taken at the 439th residue of human dystrophin (NCBI Protein Data base NP_003997), and the C terminus ends were at the 553rd and 564th residues for F114 and F125, respectively. Trp residues are situated at positions 25, 102, 108, and 112 for F114, whereas a fifth is situated at position 123 in F125. Expressed proteins were recovered as inclusion bodies from the *E. coli* expression strain and purified as described previously (28). The proteins were recovered by dispersion in 6 M guanidinium chloride, 10 mM dithiothreitol and then purified by gel chromatography in the same solvent on Sephacryl-S100. Fractions were screened by UV absorption at 280 nm and SDS-gel electrophoresis. The purified protein was kept in guanidinium chloride and dialyzed when required against the desired buffer, typically 150 mM NaCl, 50 mM sodium phosphate, pH 7.6 (buffer A). Protein concentration was determined spectrophotometrically at 280 nm using molar extinction coefficients of 23,350 and 28,570 cm^{-1} M^{-1} for F114 and F125, respectively (23).

Preparation of Phospholipidic Vesicles—Multilamellar vesicles were first prepared. Mixtures containing a 2:1 molar ratio of the lipids DOPC[2] and DOPS or DOPE in chloroform were dried overnight under vacuum and suspended in solution A containing NaCl 150 mM, EDTA 0.1 mM buffered with Tris-HCl (100 mM), pH 7.6. Small unilamellar vesicles (SUVs) were prepared extemporaneously from multilamellar vesicles diluted at 25 mg/ml and subjected to sonication at room temperature with the micro-tip of a sonicator (U200S, UKA Labortechnic) for 5 min with half-duty cycles. They were then centrifuged to eliminate titanium impurities. For fluorescence quenching experiments with membrane-bound quenchers, SUVs containing 10% brominated phosphatidylcholine (BrPSPC, dibromine palmitoylstearoylphosphatidylcholine), *i.e.* with the composition DOPC/DOPS/BrPSPC (1.9:1:0.1, M/M), were prepared. BrPSPC is commercially available (Avanti Polar, Birmingham, AL) and brominated at either 6 and 7, or 11 and 12, of the stearoyl acyl chains. For these SUVs, sonication was reduced to 1 min to avoid degradation of the spin label (29). SUVs with 10% non-brominated PSPC were used as control.

Circular Dichroism Measurements—Circular dichroism was measured (Jobin-Yvon CD6) at 281 K, with a path length of 0.02 cm and at a concentration of 50 μM protein. The percentage of molar ellipticity was calculated using a 100% α-helix coefficient of $-36{,}000$ deg·cm^2·$dmol^{-1}$ at 222 nm (23).

^{1}H NMR Spectroscopy—^{1}H NMR spectra were acquired at 500 MHz on a Bruker DMX spectrometer (11.5 teslas) equipped with a 5-mm probe (Bruker Spectrospin, Wissembourg, France). Protein concentration was 200–500 μM in the presence of 3% D_2O. Spectral width was 12 ppm, and the number of scans was 512–1024, using a repetition delay of 2 s with a 90° pulse angle. Proton decoupling sequences were used with a solvent presaturation or a WATERGATE sequence. Fourier transform was applied after a line broadening of 0.2 Hz. Chemical shifts were referenced against DSS by means of residual water resonance. Progressive magnetization transfer between water and NH protons was measured at 313 K with variable solvent presaturation delays (0.25, 0.5, 1, and 2s). The degree of magnetization transfer was estimated from the peak areas measurements.

Steady-state Fluorescence Measurements—Tryptophan fluorescence emission spectra were recorded between 320 and 450 nm using an excitation wavelength of 295 nm (bandwidth, 8.4 nm) on a SPEX 112 spectrofluorometer (Jobin-Yvon, Longjumeau, France), using a 10- × 10-mm quartz cuvette at 293 K. Blanks were always subtracted in the same experimental conditions (buffer, SUVs). Fluorescence intensities were obtained by integrating the spectra in the range 320–450 nm. Quantum yields were calculated by comparing the fluorescence intensities of the proteins with a solution of DL-Trp in buffer A, corrected to the same absorption at 295 nm (*i.e.* the excitation wavelength). A value of 0.13 was used for the quantum yield of free Trp (26).

Fluorescence quenching data were obtained with I^- (KI), Cs^+ (CsCl), 2,2,2-trichloroethanol (TCE) and acrylamide as follows: small-volume aliquots of stock solutions at 5 M of KI, CsCl, and acrylamide prepared in the protein buffer A and at 1.3 M for TCE in ethylene glycol were successively added to the samples. After each addition, the solution was gently stirred and the decrease of fluorescence intensity was measured at the initial λ_{max}. A spectrum was recorded at the end of each series to check that the quencher had no effect on the λ_{max} of the protein. As controls, KCl and ethylene glycol were shown to have no effect on the fluorescence of the proteins. Appropriate corrections for dilution were made for these experiments. The same procedure was used for quenching experiments with 5- and 16-doxyl stearoyl acids dissolved as a 20 mM stock solution in Me_2SO except that a 5-min incubation delay was allowed before data acquisition after each 1-μl addition. Effective Stern-Volmer constants (K_{sv}) were obtained from the fluorescence data according to the Stern-Volmer equation for dynamic quenching (in which collisional quenching is mainly governed by diffusion processes) (25, 26),

$$F_0/F = 1 + K_{sv}[Q], \text{ with } K_{sv} = k_q \cdot \tau_0 \qquad \text{(Eq. 1)}$$

where F_0 and F are the fluorescence intensities without and with the presence of the quencher Q, respectively, k_q is the bimolecular collisional constant, and τ_0 is the life time constant in the absence of quencher.

In the case of dynamic quenching, we obtained a linear array of points on the plots. The Stern-Volmer constant (K_{sv}) is derived from the slope of these plots. However, in some experiments, the plots deviated upward from linearity, and this could be explained by the existence of both static and dynamic quenching. Because of this, we used a modified Stern-Volmer equation (26),

$$F_0/F = (1 + K[Q])\exp^{V[Q]} \qquad \text{(Eq. 2)}$$

where K is the constant for dynamic quenching and V the constant for static quenching. Concerning quenching experiments with doxyl stearic acids, which are not soluble quenchers, "apparent" Stern-Volmer constants were calculated with Equation 1.

Titration of the Trp fluorescence emission of F125 with increasing concentrations of SUVs was effected as follows: small-volume aliquots of stock SUVs (31 mM total lipids) were successively added to F125 1 μM in a quartz cuvette. After each addition, 15 min of incubation was allowed under gently stirring before spectrum acquisition. Fluorescence intensity was determined by integrating spectra from 320 to 450 nm. Control spectra from SUVs alone were performed under the same conditions and subtracted from the respective protein spectra. When fluorescence spectra were acquired with SUVs containing brominated phosphatidylcholine, the depth of insertion was calculated using the "parallax" analysis (29, 30) with the following equation,

$$Z_{cf} = L_{c1} + [-\ln(F1/F2)/\pi C - L_{12^2}]/2L_{12} \qquad \text{(Eq. 3)}$$

where Z_{cf} is the transverse distance from the plane of the bilayer center to the plane containing the Trp residues, $F1$ and $F2$, are fluorescence intensities in presence of the shallow quencher and deeper quencher,

[1] The F125 fragment was initially assumed to be F123, as proposed by DeWolf *et al.* (4), but checking by mass spectroscopy and DNA sequence analysis showed that it is a F125 fragment, *i.e.* the carboxyl-terminal end is at the 564th residue of human dystrophin.

[2] The abbreviations used are: DOPC, 1,2-dioleyl-*sn*-glycero-3-phosphocholine; DOPS, 1,2-dioleyl-*sn*-glycero-3-phospho-L-serine; DOPE, 1,2-dioleyl-*sn*-glycero-3-phospho-L-ethanolamine; 6,7-diBrPC, 1-palmitoyl-2-stearoyl-(6,7)-dibromo-*sn*-glycero-3-phosphocholine; 11,12-diBrPC, 1-palmitoyl-2-stearoyl-(11,12)-dibromo-*sn*-glycero-3-phosphocholine; PSPC, 1-palmitoyl-2-stearoyl-*sn*-glycero-3-phosphocholine; SUVs, small unilamellar vesicles; TCE, 2,2,2-trichloroethanol; 5-DSA, 5-doxylstearic acid; 16-DSA, 16-doxylstearic acid.

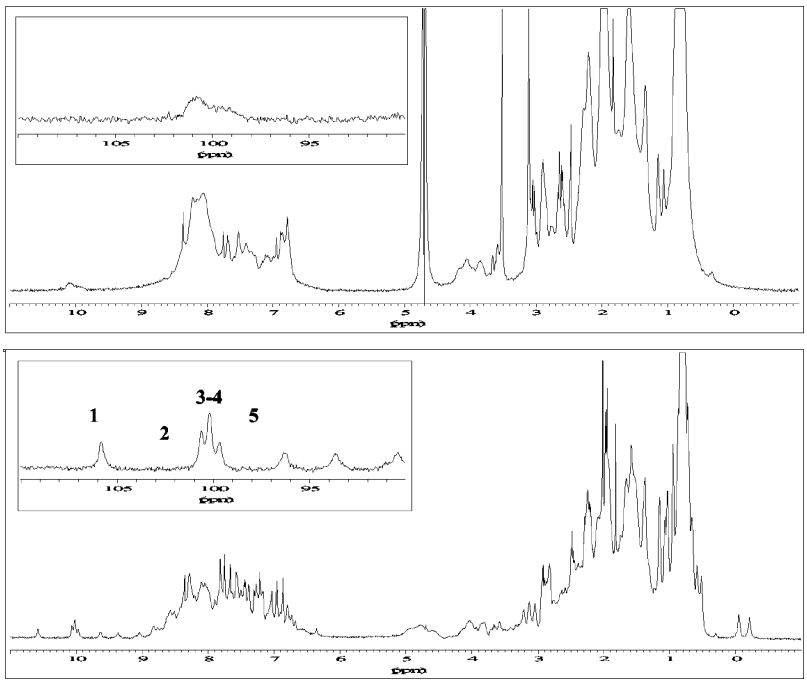

FIG. 1. **^{1}H NMR spectra of F114 and F125 at pH 7.5 recorded at 500 MHz and 298 K with the WATERGATE sequence.** The *numbers 1–5* refer to Trp residues with the Trp-1 arising at 10.6 ppm, Trp-2 at 10.08 ppm, Trp-3 and -4 at 10.0 ppm, and Trp-5 at 9.95 ppm.

respectively, L_{c1} is the transverse distance from the bilayer center to the shallow quencher, L_{12} is the transverse distance between the depths of the two quenchers, and C is the two-dimensional quencher concentration in the plane of the membrane in mole fraction of quencher lipid in total lipid per unit area. The values for the constants were L_{c1} = 10.8 Å, L_{12} = 4.5 Å for the distance between 6,7- and 11,12-diBrPC according to x-ray diffraction (31); C = (0.1)/70 Å^2, the average surface area of quencher (32). All the experimental data were fitted to the cited equations using non-linear regression analysis with Sigma-Plot software (Jandel Scientific).

Time-resolved Fluorescence Measurements—Fluorescence intensity decays were obtained by the time-correlated single photon counting technique from the $I_{vv}(t)$ and $I_{vh}(t)$ components recorded on the experimental setup installed on the SB1 window of the synchrotron radiation source Super-ACO (Anneau de Collision d'Orsay), which has been described elsewhere (33). The excitation wavelength was selected by a double monochromator (Jobin-Yvon UV-DH10, bandwidth 4 nm). An MCP-PMT Hamamatsu instrument (model R3809U-02) was used for the fluorescence measurements. Time resolution was around 20 ps, and the data were stored in 2048 channels. Automatic sampling cycles included 30-s accumulation time for the instrumental response function and 90-s acquisition time for each polarized component. The sampling was carried out such that a total number of 2–4 $\times$ 10^6 counts was attained in the fluorescence intensity decay. For measurements in the presence of SUVs, a cut-off filter (300 AELP filter, Omega Optical, Brattleboro, VT) was used to minimize contamination of the fluorescence decays by scattered excitation light. Analyses of fluorescence intensity decay as exponential sums were performed by the maximum entropy method (33).

RESULTS

Circular Dichroism Spectra—The circular dichroic spectra of the purified proteins F114 and F125 measured at 281 K exhibit molar residue ellipticities at the extremum (222 nm) of −18,000 and −30,000 deg·cm^2·dmol^{-1}, respectively. This correspond to α-helicities of 50 and 83% for F114 and F125, respectively.

^{1}H NMR Spectra—The ^{1}H NMR spectra obtained from the two proteins are shown in Fig. 1. The F114 spectrum corresponds to an only partly folded protein as indicated by the unresolved signals, particularly for the NH resonances. In contrast, the F125 spectrum displays a high chemical shift dispersion that is characteristic of folded proteins. A good marker of the tertiary structure is the presence of the two high-field shifted resonances at −0.03 and −0.19 ppm, as well as the sharp proton signals between 11.5 and 9.5 ppm. These resonances, labeled *1–5*, are assigned to the NH indole protons of the five Trp residues of F125.

The ^{1}H NMR spectra of F125 show only slight changes between 278 and 313 K (data not shown). This observation is in good agreement with the reported temperature of half denaturation of 347 K (22). Nevertheless, the signals labeled *1–5* in Fig. 1 become modified at 313 K compared with 298 K (Fig. 2). It is known that, under conditions of relatively fast exchange, hydrogen exchange rates can be measured by NMR spectroscopy to access information about the solvent accessibility and the participation of exchangeable hydrogen within hydrogen bonds (24). When using a presaturation sequence, we observe a signal decrease for several of these protons by comparison with the spectra acquired with the WATERGATE sequence (Fig. 1). This decrease of signal for some hydrogen from the NH region indicates that, at 313 K, there is an efficient magnetization transfer between water and NH protons during the presaturation delay. We therefore investigated the magnetization transfer occurring in F125 between water protons and NH protons at 313 K, using variable delays of presaturation. The results are shown in Fig. 2. It appears that there is no magnetization transfer on *peaks 1* (10.75 ppm) and *2* (10.18 ppm). By contrast, *peaks 3–5* (10.12 ppm) are strongly reduced by the presaturation of water. Because *peaks 1*, *2*, and *3–5* are derived from the five Trp residues of F125, it appears that at least two Trp residues out of five show no significant exchange with water protons at 313 K and pH 7.5. We did not attempt to study the temperature dependence of the exchange with F114, because this protein is known to have a half-denaturation temperature lower than 300 K (22).

Spectra and Decay Times of Trp Fluorescence Emission from F114 and F125—Fluorescence emission spectra acquired with an excitation wavelength of 295 nm were centered at 352 nm for F125 and at 356 nm for F114, compared with the maximum at 362 nm for a DL-Trp solution obtained in buffer A (Table I). The measured quantum yield was 0.07 and 0.05 for F114 and F125, respectively, taking a value of 0.13 for Trp in solution (34).

The fluorescence decay of each protein was also observed (see Fig. 3*A*, for an example). The curves are different for the two proteins and could not be approximated by a single-exponential

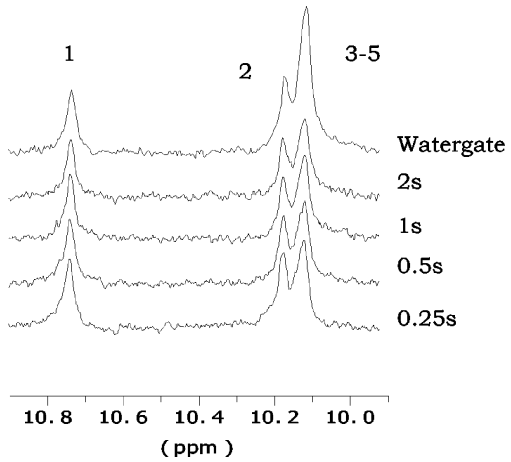

FIG. 2. **^{1}H NMR spectra of F125 at pH 7.5, 500 MHz, and 313 K.** Four spectra were acquired with a pre-saturation sequence for solvent suppression with respective delays of 0.25, 0.5, 1, and 2 s as indicated. The spectrum in the *upper part* was acquired using a WATERGATE sequence for solvent suppression.

TABLE I
Fluorescence emission spectroscopy characteristics of a DL*-Trp solution in buffer A compared to the two proteins with and without SUVs*

	λ_{max} [a]	Trp residues	Quantum yield	Average τ_0
	nm			*ns*
DL-Trp	362	1	0.13[b]	3[b]
F114	356	4	0.07	2.20
F125	352	5	0.05	1.40
F114·SUVs	352	4	0.08	2.80
F125·SUVs	342	5	0.10	2.60

[a] With excitation wavelength of 295 nm.
[b] From Ref. 34.

function. Using the maximum entropy method, the decays are well fitted by three lifetime populations for F125 and F114 (Fig. 3*B*, *upper part*). Overall, average lifetimes were calculated as 1.4 and 2.2 ns for F125 and F114, respectively (Table I). These results are in good agreement with the quantum yield values and indicate that the folded state of F125 partly "buries" some Trp residues in a more hydrophobic environment than in F114.

The anisotropy decays of each protein exhibited two different correlation time patterns (Fig. 3, *A* and *B*, *lower part*). For F125, we obtained only one correlation time at 6.8 ns (Fig. 3, *lower part*). This value is characteristic of Brownian mobility for a compact globular protein of the size of F125 (14.9 kDa). By contrast, we obtained three rotational correlation time peaks for F114 at 0.18, 1.4, and 5.2 ns (Fig. 3, *lower part*); the two shorter peaks are characteristic of the high mobility of the indole ring in the protein, whereas the longest peak is characteristic of the Brownian mobility of a protein of about 13 kDa. These results show that F125 is a structured protein, whereas F114 displays some highly mobile elements and is not as compact as F125.

As a whole, these results show that F125 is a highly structured protein compared with F114. Because of this, it could be considered as a control representing a poorly folded protein for the subsequent experiments. It was not possible to use denaturated F125 as the unfolded control, because when denaturated, F125 was not more water-soluble.

Steady-state and Time-resolved Fluorescence Quenching of Trp Emission of the Two Proteins in Aqueous Solution—Trp fluorescence quenching is a valuable method for comparing the accessibility of Trp residues to the solvent for the two studied proteins. We used Cs^+, I^-, acrylamide, and 2,2,2-trichloroethanol (TCE) as quenchers of Trp residue fluorescence.

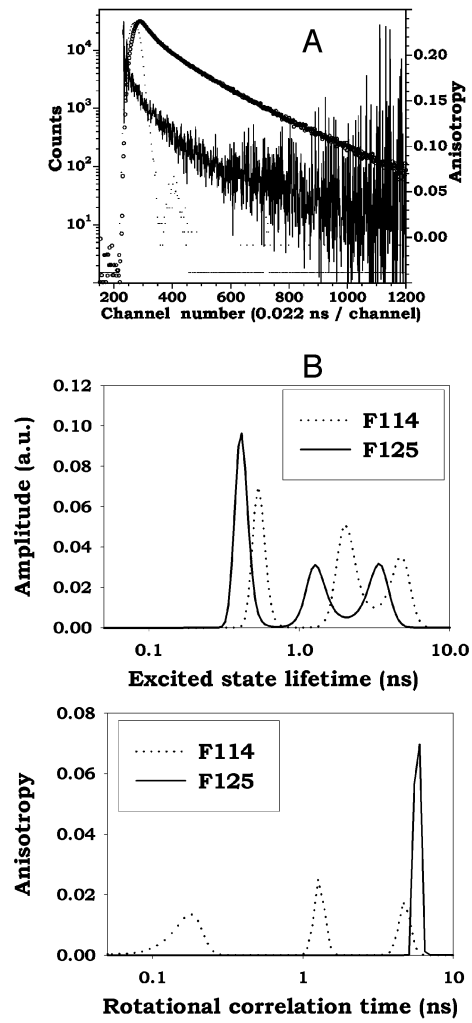

FIG. 3. *A*, experimental fluorescence intensity (*o*) and anisotropy decays (−) of Trp residues in F125. Protein concentration was 1 μM. The excitation and emission wavelengths were 295 and 350 nm, respectively. The instrumental response function is indicated as a *dotted line*. *B*, excited-state lifetime distribution profiles (*upper part*) and rotational correlation time distribution profiles (*lower part*) of Trp residues in F125 and F114. The excitation wavelength is 295 nm, and the emission wavelengths were 352 nm for F125 and 356 nm for F114. Protein concentration was 1 μM.

Quenching by I^- and Cs^+ yield linear plots of F_0/F *versus* [Q], whereas λ_{max} was unaffected by the addition of these quenchers. The dynamic apparent quenching constants K_{sv} are derived from the slopes of each of the Stern-Volmer plots (Table II). The Stern-Volmer quenching constants for Cs^+ and I^- are significantly higher for F114 than for F125. However, the bimolecular quenching constant, k_q, calculated using the average τ_0 obtained by time-resolved fluorescence, is slightly lower for F114 than for F125 (Table II). Generally speaking, these results show rather low bimolecular quenching constants compared with the values of 6–7 M^{-1} ns^{-1} for free indole derivative.

For acrylamide quenching, we found a static component for both of the proteins. The static constant, *V*, and the Stern-Volmer constant, *K*, were both significantly higher for F114 (values of 1.4 ± 0.06 and 6.5 ± 0.1 for *V* and *K*, respectively) than for F125 quenching (values of 0.9 ± 0.2 and 5.1 ± 0.4 for *V* and *K*, respectively) (results not shown).

We found no evidence of static quenching by TCE for F125, in contrast with F114 that yielded a static constant of about 3 M^{-1}. The apparent dynamic constant is very high at 20 ± 4 M^{-1} for F114 compared with 9 ± 1 M^{-1} for F125. The value of λ_{max} was

TABLE II
Trp fluorescence emission quenching of F114 and F125 in aqueous solution, and F125 in the presence of SUVs, using cesium and iodide ions and acrylamide

	Cs^+		I^-		Acrylamide	
	K_{sv} [a,b]	k_q [c]	K_{sv} [a,b]	k_q [c]	K_{sv} [d]	k_q [d]
	M^{-1}	$M^{-1}\ ns^{-1}$	M^{-1}	$M^{-1}\ ns^{-1}$	M^{-1}	$M^{-1}\ ns^{-1}$
F114	1.3 ± 0.06[e]	0.58 ± 0.03[e]	2.5 ± 0.1[e]	1.10 ± 0.12[e]	3.5	1.6
F125	1.1 ± 0.001	0.74 ± 0.03	2.0 ± 0.2	1.37 ± 0.12	3.6	2.6
F125·SUVs	0.42 ± 0.02[e]	0.15 ± 0.01[e]	0.75 ± 0.07[e]	0.29 ± 0.03[e]	2.1[e]	0.8[e]

[a] Values are expressed as mean ± S.D. for three to four identical experiments.
[b] Effective K_{sv} values are given because there is more than one Trp residue in each fragment.
[c] Calculated with the average $\langle\tau_0\rangle$ (ns) from Table I.
[d] Obtained by time-resolved fluorescence quenching.
[e] *t* test: $p < 0.05$ from F125.

unaffected by the addition of the quenchers (results not shown).

Due to the presence of static quenching observed with acrylamide and TCE, we obtained curves of τ_0/τ and the dynamic bimolecular quenching constant, k_q, from time-resolved fluorescence measurements using these quenchers. For acrylamide quenching, the curves are similar for F114 and F125 leading to K_{SV} values around 3.5 M^{-1} (Table II). These quenching constants are twice as low as those measured by steady-state fluorescence, indicating that the static quenching component cannot be accurately subtracted from the steady-state fluorescence data. The bimolecular quenching constant k_q is slightly higher for F125 compared with F114 (Table II). Overall, these results indicate a rather similar accessibility of Trp residues to acrylamide in both proteins.

By contrast, TCE quenching curves were different for the two proteins, F114 displaying a higher K_{sv} value than for F125 (Table III). These were two to three times lower than the values measured by steady-state fluorescence, indicating the existence of a much more efficient static quenching for F114 than for F125. In addition, the accessibility and exposure of Trp residues to TCE are larger in the former protein than in the latter. High values of TCE quenching have been reported for proteins known to have hydrophobic pockets able to bind small lipidic molecules such as the bovine (K_{sv} = 230 M^{-1}) or human serum albumin (K_{sv} = 20 M^{-1}) (35). This is also the case for the whole spectrin molecule with a K_{sv} value of about 20 M^{-1} (36). By contrast, the K_{sv} for F125 is similar to that obtained for acrylamide quenching, leading to the idea that Trp residues are not more accessible to TCE than to acrylamide in the folded protein F125. Such a conclusion can be drawn for most of the proteins.

Effects of Membrane Phospholipids on Trp Fluorescence Emission of Both Proteins—In a previous study, DeWolf *et al.* (10) showed that a fragment of 119 residues (F119) modified the physical properties of a model membrane containing anionic phospholipids, indicating that there was an interaction between the fragment and the phospholipids. This effect was much weaker for the fragment of 114 residues. To obtain further insight into this interaction, we incubated F125 (not used by DeWolf) and F114 with SUVs made up from the DOPC/DOPS or DOPC/DOPE 2:1 mixtures. These membrane models were chosen because the interference of fluorescence emission was minimal between Trp and these small vesicles. The incubation conditions were similar to those used by DeWolf, *i.e.* the ratio between proteins and SUV was 1 μM protein for 1.5 mM lipids, and the incubation was performed for 3 h at pH 7.5 in the presence of 0.15 M NaCl. Fig. 4*A* shows that the fluorescence intensity for F125, measured in the spectrum range between 320 and 450 nm, increases exponentially as a function of time in the presence of DOPC/DOPS SUVs. A maximum F/F_0 value of about 1.9 was observed after 3 h. At the same time, the λ_{max} shifted by 10 nm, from 352 to 342 nm (Fig. 4*B*). When DOPC/DOPE was used instead of the DOPC/DOPS mixture, there was only a very weak increase of fluorescence intensity and no λ_{max} shift (Fig. 4, *A* and *B*), indicating that the F125 fluorescence modifications upon addition of DOPC/DOPS SUVs was due to the presence of DOPS. We observed a weak effect of

TABLE III
Time-resolved Trp fluorescence quenching of the two proteins in aqueous solution and in the presence of SUVs, using TCE

	TCE	
	K_{sv}	k_q
	M^{-1}	$10^9\ M^{-1}\ s^{-1}$
F114	8.7	4
F125	3.2	2.3
F114·SUVs	15	5.4
F125·SUVs	30	11.5

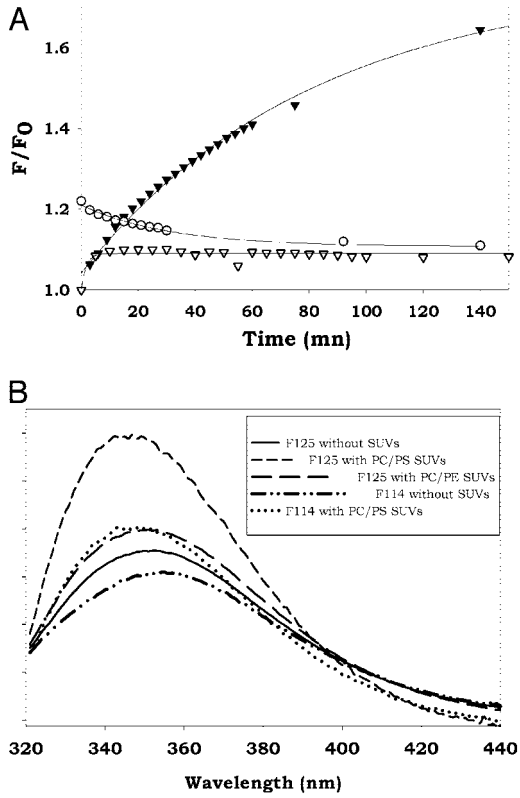

FIG. 4. *A*, time evolution of fluorescence emission of 1 μM of F125 and F114 in the presence of 1.5 mM DOPC/DOPS 2:1 (M:M) SUVs (*filled triangles* and *white circles*, respectively) and of 1 μM F125 in the presence of 1.5 mM DOPC/DOPE 2:1 (M:M) SUVs (*white triangles*). The excitation wavelength was 295 nm, with fluorescence intensity measured as the area of the spectra from 320 to 450 nm. The SUVs control spectra are subtracted from each data obtained with the proteins. *B*, fluorescence spectra of the preparations presented in *A*. Conditions were similar to *A*.

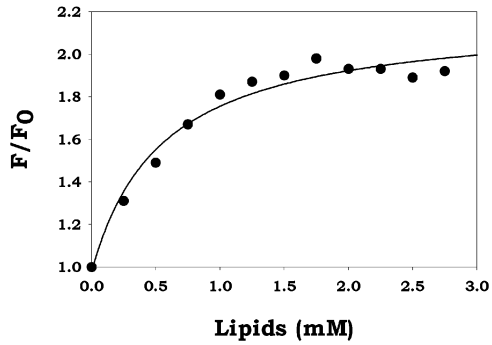

FIG. 5. **Variation of the Trp fluorescence emission of 1 μM F125 as a function of the phospholipid concentration (DOPC/DOPS 2:1 M/M).** The *line* represents the fit to a hyperbolic function.

DOPC/DOPS SUVs on F114 characterized by a rapid increase to 1.2 of the initial fluorescence and a further progressive decrease to 1.10 after three hours (Fig. 4A). The λ_{max} shifts by 6 nm from 356 nm to 350 nm (Fig. 4*B*).

We further examined the influence of an increased concentration of total lipids on the Trp fluorescence emission of F125. We acquired successive spectra of 1 μM F125 in the presence of increasing concentrations of DOPC/DOPS. Fig. 5 shows that the effect of SUVs on the Trp fluorescence intensity is subject to saturation, with a maximum fluorescence enhancement of about 1.9, as observed in Fig. 4.

The fluorescence decay of both proteins in the presence of DOPC/DOPS SUVs can be described by the sum of three exponential components (Fig. 6), whereas the average lifetimes τ_0 in the presence of SUVs are calculated as 2.6 and 2.8 ns for F125 and F114 (Table I), respectively. Thus, upon interaction with anionic SUVs, the lifetime for F125 increases by 85% as against 27% for F114. This is in agreement with the increases in the fluorescence intensities observed under these conditions.

All these modifications of F125 Trp fluorescence in the presence of anionic SUVs are indicative of a more hydrophobic environment of the Trp residues. This suggests either the existence of contacts in the vicinity of the indole rings between the protein F125 and the membrane lipids (26), or a conformational change burying most of the Trp residues inside the protein. Either of these effects is likely to be very moderate for F114. Thus, the effects of the presence of anionic SUVs appear to be much more specific in the case of the more structured protein.

Effects of SUVs on Trp Fluorescence Quenching of F125—The existence of contacts between Trp residues and membrane lipids implies that the accessibility of Trp residues in F125 in the presence of anionic SUVs must be decreased compared with free F125. The accessibility of Trp residues in F125 in the presence of DOPC/DOPS SUVs was therefore explored here by fluorescence quenching. Steady-state fluorescence quenching was carried out using Cs^+, I^-, and acrylamide. The K_{sv} values for Cs^+ quenching decrease by 40% for F125 incubated with DOPC/DOPS SUVs compared with the protein alone, yielding a bimolecular quenching constant more than five times lower than in the absence of membrane phospholipids (Table II). The same result holds for I^- and acrylamide quenching, with bimolecular quenching constants decreasing about 5-fold and more than 3-fold, respectively, in the presence of DOPC/DOPS SUVs as compared with aqueous solution (Table II). Thus, it appears that the presence of SUVs strongly decreases the exposure of the Trp to these quenchers, arguing for a close proximity of the Trp to the membrane surface that is generally able to shield Trp residues from the solvent.

The bimolecular quenching constant of TCE for F125 in the

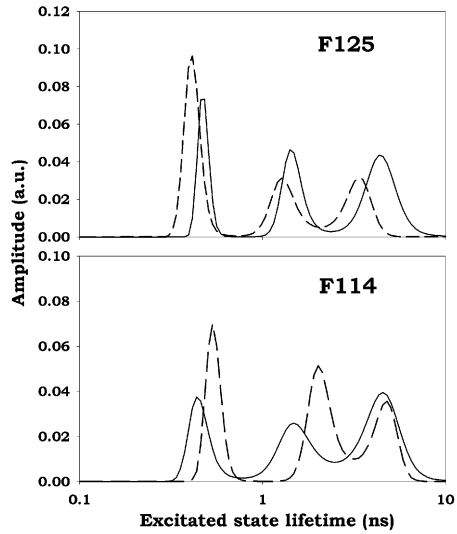

FIG. 6. **Excited-state lifetime of Trp residues in F125 (*upper part*) and F114 (*lower part*) after 3-h incubation with 1.5 mM SUVs (DOPC/DOPS 2:1, M/M) (*solid lines*).** For comparison, the profiles obtained without SUVs in Fig. 3 are shown (*dashed lines*). The excitation wavelength was 295 nm, whereas the emission wavelengths were 342 and 350 nm for F125 and F114, respectively. Protein concentration was 1 μM.

presence of DOPC/DOPS SUVs is five times higher than in water (Table III). This enhanced quenching by TCE is also observed by steady-state fluorescence, where the K_{sv} values are 13 and 64 M^{-1} for F125 in aqueous solution and in the presence of DOPC/DOPS SUVs, respectively (data not shown). A large static component is revealed by the discrepancies between the K_{sv} measured by steady-state and time-resolved fluorescence. The explanation for this enhanced quenching by TCE is as follows: TCE partitions into the lipid bilayer, where it senses the hydrophobic environment and efficiently quenches the Trp residues that occur in this hydrophobic environment. These results clearly indicate that the environment of the Trp residues is highly hydrophobic when F125 is in the presence of DOPC/DOPS SUVs.

We also checked the TCE partitioning within hydrophobic volumes such as membrane systems using a model system of dodecyl-maltoside micelles that comprise a long-tailed tryptophan derivative, the tryptophanyl-octyl ester. The fluorescent moiety of this ester is known to be located at the polar-hydrophobic interface (37). The k_q value associated with tryptophanyl-octyl ester quenched by TCE was measured at 19 M^{-1} ns^{-1}. This is six times higher than the value for the water-soluble derivative *N*-acetyl-tryptophanamide, which yielded a value of 3 M^{-1} ns^{-1} (results not shown). These results confirm those obtained with F125 in the presence of DOPC/DOPS SUVs.

In addition, by comparing this strong effect of TCE on F125 in the presence of DOPC/DOPS SUVs, we can see that the k_q value obtained by time-resolved fluorescence of F114 was not modified by the presence of these SUVs (Table III). This demonstrates that Trp fluorescence of F114 is unaffected by SUVs and, thus, that the strong effect of the presence of DOPC/DOPS SUVs on F125 is specific of a structured protein. The overall results from TCE quenching show that the Trp residues of F125 in the presence of DOPC/DOPS SUVs are in a more hydrophobic environment than in F125 in aqueous solution and are probably in close proximity to the membrane lipids.

Trp Fluorescence Quenching of F125 with Membrane-bound Quenchers—Additional support for the close proximity of F125 to the membrane lipids comes from two other data on quenching of fluorescence with lipids brominated or spin-labeled at

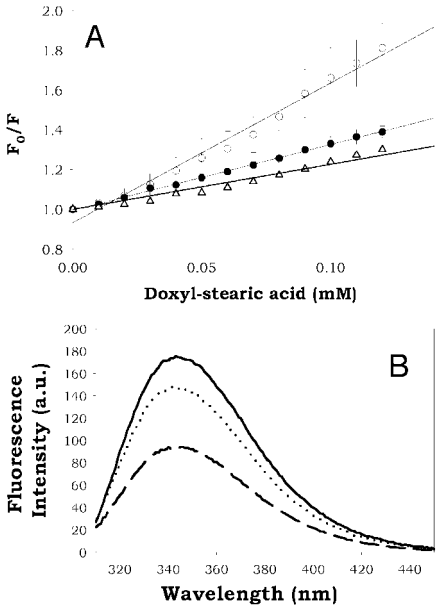

FIG. 7. *A*, Stern-Volmer plots of quenching of tryptophan fluorescence in F125 1 μM in the presence of 1.5 mM SUVs by doxyl stearic acids. Increasing concentrations of 5-doxyl and 16-doxyl stearic acids (*white* and *black circles*, respectively) were added to F125 in the presence of anionic DOPC/DOPS SUVs. As a control, 5-doxyl stearic acid was added to F125 in the presence of zwitterionic DOPC/DOPE SUVs (*white triangles*). Excitation wavelength was 295 nm, and emission wavelength was 342 nm. A plot of F_0/F *versus* doxyl stearic acids yields a *line* where the slope is the apparent Stern-Volmer constant. *B*, fluorescence spectra of 0.2 μM F125, in the presence of 1 mM DOPC/DOPS 2:1 SUVs where DOPC was substituted for 10% by palmitoyl-stearoyl-phosphatidylcholine non-brominated (*solid line*) or brominated in positions 11 and 12 (*dotted line*) or 6 and 7 (*dashed line*), were recorded between 300 and 450 nm. Excitation wavelength was 295 nm.

different positions on the acyl chain, *i.e.* 5-doxyl and 16-doxyl stearic acid and 6,7-diBrPC- and 11,12-diBrPC-containing SUVs. Because these lipids are membrane-bound quenchers, comparison of their respective quenching ability yields information about the relative location of the tryptophan residues compared with the surface of the bilayer.

With 5-doxyl and 16-doxyl stearic acid (Fig. 7*A*), calculation of the apparent Stern-Volmer constant revealed that 5-DSA, with an apparent Stern-Volmer constant of 7 ± 1 mM^{-1}, was 2-fold more effective in quenching fluorescence than 16-DSA, with a constant value of 3.3 ± 0.2 mM^{-1}. As a control, 5-DSA quenched weakly the fluorescence of Trp of F125 in presence of SUVs composed of zwitterionic SUVs, with an apparent Stern-Volmer constant of 2.3 mM^{-1}. This leads us to conclude that Trp residues of F125 in the presence of anionic SUVs are very close to the surface of the bilayer.

A similar conclusion came from experiments where F125 was incubated with SUVs comprising 10% of brominated PC (Fig. 7*B*). It appears that the presence of brominated phospholipids in the vesicles induced significant quenching of the Trp fluorescence in F125. The magnitude of the quenching is higher when the bromine atoms are located in positions 6 and 7 of the acyl chain with 42% of quenching efficiency, than when present at positions 11 and 12 with 16% of quenching efficiency, and is consistent with a location of the protein close to the shallow quencher. We attempted to calculate the depth of penetration of Trp residues by the "parallax" method, according to the expression given under "Materials and Methods," being aware that the computed value of Z_{cf} is an average over the five Trp residues of the F125. A value of 18.5 Å is obtained for the distance between the Trp and the center of the bilayer. The main conclusion is that the protein Trp residues are, on the average, located closer to the membrane/water interface than the 6 to 7 bromine atoms. We thus conclude that the protein is lying along the membrane surface with several Trp residues very close to the polar head groups of the phospholipids.

DISCUSSION

The function of the rod domain of dystrophin, which is made up of 24 spectrin-like repeats, remains unresolved. Two interesting observations indicate that some central basic repeats bind to F-actin (6) and that the second repeat may interact with artificial membrane containing phosphatidylserine (10). This latter observation provides some clues about the targeting of the dystrophin onto the sarcolemma. Thus, it remains important to determine the nature of the interaction between membrane phospholipids and the dystrophin rod domain. We need to determine whether the Trp residues (five in the second repeat) are involved in the interaction. The present study supports the view that Trp residues become located at the water-membrane interface in the complex protein-membrane and that this process concerns only the folded protein F125.

Various lines of experimental evidence demonstrate that the longer protein (F125) is more folded than the shorter (F114). The high chemical shift dispersion in the ^{1}H NMR one-dimensional spectrum and the higher fluorescence maximum emission intensity, as well as the shorter excited-state lifetime and the blue shift of the Trp fluorescence emission of F125 compared with F114, all indicate that the Trp residues of F125 are more shielded from the surface than in the case of F114. This view is accepted as the general rule for folded proteins (26). The anisotropy decay confirms that F125 is more compact and structured than F114.

Overall, the fluorescence quenching data reported here indicate that both of the proteins in aqueous solution are characterized by structural fluctuations. In fact, all the Trp residues in F125 and F114 appear to be accessible to fluorescence quenchers. The lower quenching efficiency of the Cs^+ ions compared with the I^- ions is consistent with a preferential cationic environment for the Trp residues in both proteins. The acrylamide bimolecular quenching constants, rather similar for F125 and F114, are of the same order of magnitude as that found for a Trp residue in a random coil polypeptide (38) as well as for Trp in entire spectrin (36) and in a repeat of the c-Myb protein (39). These two last proteins display a coiled-coil type structure (39, 40) as also assumed for the repeats of the dystrophin rod domain (2, 22, 41). This indicates that the Trp residues of coiled-coil proteins may be relatively easily accessible to acrylamide. By contrast, the accessibility of the studied proteins to acrylamide is one order of magnitude higher than that reported for domain III of Annexin V, a globular protein with a Trp residue deeply buried in the protein matrix (42). In coiled-coil proteins, Trp are accessible either because of the structure of the protein, which could be the case for the compact folded F125, or, alternatively, due to large internal motions that could be the case for the non-structured F114.

Finally, the non-polar TCE quenches the fluorescence of Trp residues in close proximity to hydrophobic sites at the surface of the proteins (35, 36). Thus, it is a more effective quencher for F114 than for F125, indicating that the surface of the folded protein F125 is relatively less hydrophobic than F114.

Several strong changes occur when F125 is in the presence of model membranes made up partly of anionic phosphatidylserine. On the other hand, very weak changes are observed for F114 with SUVs or for F125 with zwitterionic SUVs. In the presence of anionic SUVs, the maximum intensity of the fluorescence emission spectrum is increased and shifted toward shorter wavelengths compared with the free F125 pro-

tein, indicating that the Trp residues are located in a more hydrophobic environment in the complex F125·SUVs (43–47). In fact, this modified localization of the Trp residues could be due either to the close proximity of indole rings to the membrane phospholipids or to a protein conformational change that is able to bury the Trp residues from the surface. However, the latter effect would be accompanied by a shortening of the fluorescence excited-state lifetime of the Trp emission as is often observed in structured proteins (26). This is not the case here, because the excited-state lifetime is largely increased in the complex F125·SUVs compared with the free F125, in agreement with the 2-fold increase of fluorescence intensity. Such observations are the general rule when Trp residues are close to the surface of the lipid membrane and not fully exposed to the aqueous solvent. This indicates clearly that the more hydrophobic environment encountered by Trp in the complex F125·SUVs is produced by the close proximity of the Trp to the membrane surface (42). It is noteworthy that these large modifications are restricted to the highly folded repeat F125, because the poorly structured protein F114 detects only a very weak modification when in the presence of SUVs.

The large decrease of Trp fluorescence quenching by ions and acrylamide observed in the complex F125·SUVs compared with the free F125 shows that the Trp residues are shielded from the solvent and confirms the localization of Trp residues at the membrane surface. By contrast, we see a large increase in the TCE quenching of Trp residues in the F125·SUV complex. Because TCE have the property of partitioning into hydrophobic pockets at the surface of proteins, where it dynamically quenches the fluorescence emission, the quenching is enhanced in a hydrophobic environment (35). The 6-fold increase in the bimolecular TCE quenching constant of Trp residues in the F125·SUV complex thus shows that the Trp residues are in a highly hydrophobic environment. Overall, our observations clearly suggest that the formation of a complex between F125 and SUVs leads to a shielding of Trp residues from the aqueous solvent by a mechanism that places them in close contact with the membrane phospholipids.

Trp residues in membrane or peripheral proteins tend to cluster near to or at the lipid-water interface of the membrane (20, 48). In membrane proteins, Trp residues are mostly located in extramembranal segments lying parallel to the surface of the membrane. Aromatic residues such as Trp, Tyr, and Phe are known to be particularly suitable for interfacial positioning, because they can effectively bridge the gap between the two contrasting environments existing at the membrane-water interface (19, 49). In the repeat of the dystrophin rod domain, it is likely that several Trp residues are also accommodated at the lipid-water interface. This is strongly supported by the data obtained with membrane-bound quenchers. The fact that these compounds are effective quenchers showed that the Trp residues are not far from these quenchers. In addition, the quenching efficiency was more pronounced with the shallow quenchers, 5-DSA and 6,7-diBrPC, than with the deeper quenchers, 16-DSA and 11,12-diBrPC, indicating unequivocally that the Trp residues are, on the average, located at the surface of the bilayer. Four out of the five Trp residues of F125 are situated in the presumed third helix of the repeat, so we infer that the repeat lies along the surface of the membrane bilayer. However, Trp fluorescence modifications are not observed for SUVs prepared with zwitterionic phospholipids alone, *i.e.* when no net charges are present at the membrane surface. This suggests that hydrophobic interactions between Trp residues and the membrane lipids are not the driving force behind the formation of the F125·SUV complex. It is likely that electrostatic attractions play a role in the initiation of complex formation, which could then be stabilized by both hydrophobic and electrostatic forces as in the case of many peripheral membrane proteins (48). Dystrophin may thus be classified in the important family of lipid-binding cytoskeletal proteins, which includes vinculin, spectrin, and talin, proteins also known to bind other cytoskeletal proteins (actin, α-actinin, and integrins) to form complex structural arrays (50).

Finally, our study stresses the potential role of the rod domain of dystrophin in targeting onto the sarcolemma, even when the carboxyl-terminal end is absent as observed in patients with genetic variants lacking this end (11–13). Furthermore, the presence of several repeats and hinges is essential for a complete rescue of the *mdx* phenotype (14, 51). The dystrophin molecule appears to be involved in an important array situated at the sarcolemma, comprising not only cytoskeletal proteins (5, 6, 52) and membrane proteins (53–56) but also membrane phospholipids.

Acknowledgments—We gratefully acknowledge W. B. Gratzer for providing the plasmids and J. P. Douliez for acquisition of circular dichroism spectra. We thank F. Toma for stimulating discussions. M. S. N. Carpenter post-edited the English style.

REFERENCES

1. Hoffman, E. P., Brown, R. H., and Kunkel, L. M. (1987) *Cell* **51,** 919–928
2. Koenig, M., Monaco, A. P., and Kunkel, L. M. (1988) *Cell* **53,** 219–226
3. Ervasti, J., and Campbell, K. (1991) *Cell* **66,** 1121–1131
4. Campbell, K. P. (1995) *Cell* **80,** 675–679
5. Ervasti, J. M., Rybakova, I. N., and Amann, K. J. (1997) *Soc. Gen. Physiol.* **52,** 31–44
6. Amann, K. J., Renley, B. A., and Ervasti, J. M. (1998) *J. Biol. Chem.* **273,** 28419–28423
7. Ervasti, J., and Campbell, K. (1993) *Curr. Opin. Cell Biol.* **5,** 82–87
8. Brown, S. C., and Lucy, J. A. (1993) *Bioessays* **15,** 413–419
9. Rybakova, I. N., Patel, J. R., and Ervasti, J. M. (2000) *J. Cell Biol.* **150,** 1209–1214
10. DeWolf, C., McCauley, P., Sikorski, A. F., Winlove, C. P., Bailey, A. I., Kahana, E., Pinder, J. C., and Gratzer, W. B. (1997) *Biophys. J.* **72,** 2599–2604
11. Hoffman, E., Carlos, P., Garcia, A., Chamberlain, J., Angelini, P. C., Lupski, J., and Fenwick, R. (1991) *Ann. Neurol.* **30,** 605–610
12. Helliwell, T., Ellis, J., Mountford, R., Appleton, R., and Morris, G. (1992) *Am. J. Hum. Genet.* **50,** 508–514
13. Recan, D., Chafey, P., Leturcq, F., Hugnot, J., Vincent, N., Tome, F., Collin, H., Simon, D., Czernichow, P., Nicholson, L., Fardeau, M., Kaplan, J., and Chelly, J. (1992) *J. Clin. Invest.* **89,** 712–716
14. Harper, S. Q., Hauser, M. A., DelloRusso, C., Duan, D., Crawford, R. W., Phelps, S. F., Harper, H. A., Robinson, A. S., Engelhardt, J. F., Brooks, S. V., and Chamberlain, J. S. (2002) *Nat. Med.* **8,** 253–261
15. Sikorski, A. F., Michalak, K., Bobrowska, M., and Kozubek, A. (1987) *Studia Biophysica* **121,** 183–191
16. Diakowski, W., Prychidny, A., Swistak, M., Nietubyc, M., Bialkowska, K., Szopa, J., and Sikorski, A. F. (1999) *Biochem. J.* **338,** 83–90
17. O'Toole, P. J., Morrison, I. E. G., and Cherry, R. J. (2000) *Biochim. Biophys. Acta* **1466,** 39–46
18. Manno, S., Takakuwa, Y., and Mohandas, N. (2002) *Proc. Natl. Acad. Sci. U. S. A.* **99,** 1943–1948
19. Yau, W.-M., Wimley, W. C., Gawrisch, K., and White, S. H. (1998) *Biochemistry* **37,** 14713–14718
20. Killian, J. A., and von Heijne, G. (2000) *Trends Biochem. Sci.* **25,** 429–434
21. Clayton, A. H., and Sawyer, W. H. (2000) *Biophys. J.* **79,** 1066–1073
22. Calvert, R., Kahana, E., and Gratzer, W. B. (1996) *Biophys. J.* **71,** 1605–1610
23. Kahana, E., and Gratzer, W. B. (1995) *Biochemistry* **34,** 8110–8114
24. Dempsey, C. (2001) *Prog. Nucl. Magn. Res. Spect.* **39,** 135–170
25. Eftink, M. R., and Ghiron, C. A. (1981) *Anal. Biochem.* **114,** 199–227
26. Lakowicz, J. (1999) *Principles of Fluorescence Spectroscopy*, Kluwer Academic, Norwell, MA
27. Wimley, W. C., and White, S. H. (2000) *Biochemistry* **39,** 161–170
28. Kahana, E., Marsh, P. J., Henry, A. J., Way, M., and Gratzer, W. B. (1994) *J. Mol. Biol.* **235,** 1271–1277
29. Abrams, F., and London, E. (1992) *Biochemistry* **31,** 5312–5322
30. Chattopadhyay, A., and London, E. (1987) *Biochemistry* **26,** 39–45
31. McIntosh, T., and Holloway, P. (1987) *Biochemistry* **26,** 1783–1788
32. Lewis, B., and Engelman, D. (1983) *J. Mol. Biol.* **166,** 211–216
33. Vincent, M., Gallay, J., and Demchenko, A. (1995) *J. Phys. Chem.* **99,** 14931–14941
34. Lakowicz, J. R. (1983) *Principles of Fluorescence Spectroscopy*, Plenum Press, New York and London
35. Eftink, M. R., Zajicek, J. A., and Ghiron, C. A. (1977) *Biochim. Biophys. Acta* **491,** 473–481
36. Kahana, E., Pinder, J. V., Smith, K. S., and Gratzer, W. B. (1992) *Biochem. J.* **282,** 75–80
37. De Foresta, B., Gallay, J., Sopkova, J., Champeil, P., and Vincent, M. (1999) *Biophys. J.* **77,** 3071–3084
38. Eftink, M. R., and Ghiron, C. A. (1976) *Biochemistry* **15,** 672–680

39. Zargarian, L., Tilly, V. L., Jamin, N., Chaffotte, A., Gabrielsen, O., Toma, F., and Alpert, B. (1999) *Biochemistry* **38,** 1921–1929
40. Pascual, J., Pfuhl, M., Walther, D., and Saraste, M. (1997) *J. Mol. Biol.* **273,** 740–751
41. Cross, R. A., Stewart, M., and Kendrick-Jones, J. (1990) *FEBS Lett.* **262,** 87–92
42. Sopkova, J., Vincent, M., Takahashi, M., Lewit-Bentley, A., and Gallay, J. (1999) *Biochemistry* **38,** 5447–5458
43. Dufourcq, J., and Faucon, J. F. (1977) *Biochim. Biophys. Acta* **467,** 1–11
44. Köhler, G., Hering, U., Zschörnig, O., and Arnold, K. (1997) *Biochemistry* **36,** 8189–8194
45. Vogt, T. C. B., and Bechinger, B. (1999) *J. Biol. Chem.* **274,** 29115–29121
46. Saurel, O., Cezanne, L., Milon, A., Tocanne, J.-F., and Demange, P. (1998) *Biochemistry* **37,** 1407–1410
47. Schmitz, A., Ulrich, A., and Vergères, G. (2000) *Arch. Biochem. Biophys.* **380,** 380–386
48. De Planque, M. R., Kruijtzer, J. A., Liskamp, R. M., Marsh, D., Greathouse, D. V., Koeppe, R. E., de Kruijff, B., and Killian, J. A. (1999) *J. Biol. Chem.* **274,** 20839–20846
49. Yuen, C. T., Davidson, A. R., and Deber, C. M. (2000) *Biochemistry* **39,** 16155–16162
50. Niggli, V. (2001) *Trends Biochem. Sci.* **26,** 604–611
51. Tinsley, J., Deconinck, N., Fisher, R., Kahn, D., Phelps, S., Gillis, J.-M., and Davies, K. (1998) *Nat. Med.* **4,** 1441–1444
52. Rybakova, I., and Ervasti, J. (1997) *J. Biol. Chem.* **272,** 28771–28778
53. Campbell, K., and Kahl, S. (1989) *Nature* **338,** 259–262
54. Ohlendieck, K., Ervasti, J. M., Snook, J. B., and Campbell, K. P. (1991) *J. Cell Biol.* **112,** 135–148
55. Ervasti, J., and Campbell, K. (1993) *J. Cell Biol.* **122,** 809–823
56. Straub, V., and Campbell, K. P. (1997) *Curr. Opin. Neurol.* **10,** 168–175